Self-Modeling Curve Resolution Analysis of On-Line Vibrational Spectra of Polymerisation and Transesterification

Yukihiro Ozaki, Slobodan Šašić, and Jian-Hui Jiang*

Department of Chemistry, School of Science, Kwansei Gakuin University, Gakuen, Sanda, Hyogo 669-1337, Japan

Heinz W. Siesler

Department of Physical Chemistry, University of Essen, D-45117, Essen, Germany

Summary: This article discusses the potential of self-modeling curve resolution analysis (SMCR) for the evolution of on-line vibrational spectral data of polymerisation and transesterification. After the general introduction of the SMCR approach, representative SMCR techniques like orthogonal projection analysis (OPA) and simple-to-use interactive self-modeling mixture analysis (SIMPLISMA) are briefly outlined. As examples the SMCR analysis of the Raman spectra of the block copolymerisation of styrene and 1,3-butadiene and that of the near-infrared (NIR) spectra of the melt-extrusion transesterification of ethylene-vinylacetate copolymer will be illustrated. In the last part of this review paper, a new powerful SMCR method that we have recently proposed is demonstrated.

INTRODUCTION

Vibrational spectroscopic monitoring of reactions and processes has recently received great interest in industries.[1-5] rapid progress in various types of detectors, optical systems, fiber optics, and optical filtering designs has significantly improved the performance of vibrational spectroscopy. The advantages of vibrational spectroscopy in process analysis are, for example, nondestructive and in-situ monitoring of physical and chemical process parameters. The real-time monitoring of a reaction system by vibrational spectroscopy enables one to make qualitative and quantitative analysis of the components in the system. However, the vibrational spectroscopic data collected during on-line monitoring are often complicated and their analysis is not always straightforward. Up to now, various multivariate analysis methods have been employed

 CCC 1022-1360/00/$ 17.50+.50/0

in vibrational spectroscopic process analysis among which the calibration-based methods seem to be most important.[1-5] The popularity of calibration methods is especially notable in the field of vibrational spectroscopy. However, these the methods fail whenever one is not able to develop a model for a given reaction due to lack of knowledge of the reference concentrations or other type of data important for the calibration.

Recently, there has been increasing interest in self-modeling curve resolution (SMCR) methods for on-line chemical reactions because the SMCR methods can address the problems that the calibration-based methods have.[6-9] The SMCR approach enables one to resolve the experimental matrix into concentration profiles and pure spectra of the involved species without prior knowledge of these features. Although SMCR methods have been employed mainly in the field of chromatography, recently several research groups have reported successful applications of SMCR methods to vibrational spectroscopy. For example, Tauler et al.[6,7] studied the application of SMCR to IR spectra acquired during several process runs and for monitoring the Fujiwara reaction. Šašić et al.[12] reported SMCR analysis of on-line near-infrared (NIR) spectra of the melt-extrusion transesterification of ethylene-vinylacetate copolymer. Bandermann et al.[13] used SMCR to analyze Fourier-transform (FT) Raman spectroscopic on-line monitoring of the anionic dispersion block copolymerisation of styrene and 1,3-butadiene.

The purpose of this article is to review the recent progress in SMCR analyses of on-line Raman spectra of polymerisation. The first part of this review is concerned with the outline of the theory of SMCR methods. In the second part we show examples of SMCR studies of on-line Raman spectra of a polymerization reaction and on-line near-infrared (NIR) spectra of a transesterification reaction. The last part introduces a new SMCR approach that we have recently developed.[14-16]

SELF MODELING CURVE RESOLUTION

In terms of the uniqueness of the solution, SMCR techniques can be divided into two types. Techniques of the first type look for a unique resolution where the factors for single species are uniquely defined according to the mathematical principle involved. Typical approaches for unique resolution consist of evolving factor analysis (EFA),[17]

window factor analysis (WFA),[18] heuristic evolving latent projection (HELP),[19,20] subwindow factor analysis (SFA)[21] and parallel vector analysis (PVA).[14-16] To combat the so-called rotational ambiguity intrinsic in two-way resolution, these techniques have to inspect the evolving behavior of the components using some evolutionary rank analysis methods and utilize certain feature regions such as selective regions or zero-concentration regions.

The second type of techniques aim at finding a rational resolution in which the factors for single species do not violate any *a priori* knowledge such as non-negativity and unimodality. In principle, rational resolution produces a set of feasible solutions. The accuracy of the solution depends on the correlation among the pure profiles underlying the two-way data. When the correlation among the pure profiles is not very severe, rational resolution can give solutions approximating very well the true profiles. Routine techniques for rational resolution comprise orthogonal projection analysis (OPA),[22,23] simple to use interactive self-modeling mixture analysis (SIMPLISMA),[23-25] iterative target transformation factor analysis (ITTFA),[26,27] positive matrix factorization (PMF),[28] alternating least squares (ALS)[29] and elementary matrix transformation-based procedures.[30] These methods can be differentiated from each other in the start estimates and the iteration procedures. A good start approximating the true profiles as well as possible usually yields improved resolution while an efficient optimization algorithm is expected to show fast convergence.

THEORY

In this section we describe briefly the basic postulates behind the SMCR methods. In a spectral system that obeys Beer's law, the data matrix X consisting of m samples (spectra) and n variables (wavenumbers) can be written as;

$$X=CS^t \tag{1}$$

where C (dimension m x c) is a matrix of species concentrations aligned in columns while S (dimension n x c) is a matrix of species spectra aligned in columns. The goal of an SMCR analysis is to determine the matrices C and S. The first step to do is to find c, the number of components present in the system. After that, one needs to determine

samples or variables where only one component contributes. If there are some columns of X (selective variables) where only contributions from *c* different species exist, then C can be approximated by these columns and pure component spectra can be obtained by a least-squares procedure;

$$S^t = (C^tC)^{-1}C^tX \quad (2)$$

In chromatography it is possible to find some selective retention times that represent pure component spectra, and then pure concentration profiles can be approximated by:

$$C = XS(S^tS)^{-1} \quad (3)$$

In what fellows the theory of representative SMCR methods will be described briefly.

Simplisma

Simplisma searches for the 'pure variables' that are actually wavenumbers where only one component in the system gives a spectral response.[23,24] After determining the pure variables representing all the species in the system, one can apply eq. (3) to calculate the corresponding pure species spectra because the intensity changes in the pure variables are proportional to the concentration changes and, if aligned in separate columns, form matrix C. In Simplisma the first pure variable is identified as the one along which the ratio of standard deviation to the mean of the intensity changes is largest. The higher pure variables fulfil the above condition and are additionally orthogonal to the previously found pure variables.

OPA

OPA, originally developed by Cuesta Sanchez et al.,[22] may be the simplest SMCR method because it does not require any pre-treatment of the original data and is intuitively easy to understand. OPA searches for the variables along which exclusively one component has a spectral response or alternatively for the samples where only one component exists. Once such variables (or samples) are found, the corresponding pure component concentration profiles or the pure component spectra can be easily calculated by the least squares regression. The pure component spectra may be

estimated by eq. (2) while if the pure samples (i.e. pure component spectra) are determined, then the pure component concentration profiles may be estimated by eq. (3). In OPA pure variables (samples) are considered to be the vectors in the space of the experimental data that are geometrically furthest from each other. The angles between variables (samples) are measured by calculating series of determinants of 2x2 cross product matrices that are made up from all possible pairs of variables (samples).

HELP

Help reveals pure variables as those that lie on a straight line passing through the origin of the space spanned by the principal components (PC_S).[19,20] If the variables are pure, then they are separated only by a scaling factor (number). Consequently, they must lie on a line. If in the PC1 vs. PC2 score or loading plot one can draw straight lines that pass through the origin, then these variables present regions of high selectivity i.e. the variables (samples) are pure or are those closest to the pure variables.

ITTFA

This method was proposed in 1984 and thus has been investigated in more detail than other methods.[26,27] The first step of ITTFA starts with a target vector **t** (1 x *m*) that is suspected to have the shape of the pure-component concentration profile. Then, the target is projected onto the space defined by important eigenvectors of **X** by

$$\mathbf{p}=\mathbf{t}\mathbf{U}^{t}\mathbf{U} \qquad (4)$$

where **p** is a projected vector and **U** is a c x *m* matrix of score eigenvectors. **p** must be a physically reasonable vector. It cannot contain negative values and should have only one maximum (unimodality). If **p** does not meet these conditions, then its values are iteratively changed. Negative coordinates are set to zero and the changed **p** becomes the new target **t**. That target is again projected by eq. (4), producing new **p** that is tested to its identity to **t**. The process continues until the difference between **p** and **t** becomes less than some threshold value. As initial **t** one can use results of Varimax rotation or needle search. The constraints of non-negativity must be fulfilled in all the cases, while the constraint of unimodality is not so strict and is usually important in chromatography. After determining *c* vectors that satisfy these conditions, pure component spectra can be determined by eq.(2).

SELF-MODELING CURVE RESOLUTION ANALYSIS OF ON-LINE RAMAN DATA OF POLYMERISATION

As an example of an SMCR analysis of on-line Raman spectra, this review paper describes the successful application of light-fibre FT-Raman spectroscopy to monitor the progress of the (styrene-butadiene-styrene)-triblockcopolymerisation.[13] Monitored is the process of styrene/1,3-butadiene block-copolymerisation that yields industrially important material but whose real-time evolution has not yet been satisfactorily charted. The reaction of styrene-butadiene copolymerisation is performed as heterogeneous anionic dispersion polymerisation in an aliphatic continuous phase.[13] The obtained products are of spherical sizes whose dimensions can be controlled by experimental conditions. Heterogeneity of the reaction and turbulent phase fluctuations make the monitoring of the process very demanding. Most of the conventional analytical techniques are not efficient enough to probe this type of tailor-made polymerisation and are definitely not suitable for the on-line monitoring.[13] Therefore, this system is probably an excellent target for SMCR coupled with light fibre-FT-Raman spectroscopy.

The experimental details for the copolymerisation procedure were described elsewhere.[31] The experimental set-up for the Raman measurements combined with the polymerization procedure were reported in our previous paper.[13] During the initial styrene polymerisation FT-Raman spectra were collected in about 2 min intervals by accumulating 114 scans at a spectral resolution of 4 cm^{-1}. After 50%(w/w) styrene bad polymerised butadiene was added and the time interval between spectra acquisition was increased to about 4 min and 228 scans were accumulated at the same spectral resolution. Prior to the SMCR analysis the spectra were subjected to a multiplicative scatter correction (MSC) for correcting baseline changes.

Fig. 1 shows the FT-Raman spectra in the 1700-1620 cm^{-1} region acquired during the polymerisation.[13] Raman bands at 1639 and 1632 cm^{-1} are due to 1,3-butadiene and monomeric styrene, respectively. Weak features in the 1680-1650 cm^{-1} region arise from the different configurational isomers (1,4-cis and 1,4-trans) of the evolving poly(butadiene) blocks. In the 1700-1620 cm^{-1} region, only contributions of styrene, 1,3-butadiene, and poly(butadiene) are present. Therefore, the spectra are

considered to be a sum of the contributions of these species.[13]

$$\mathbf{X}=C_S\mathbf{S}_S^T+C_B\mathbf{S}_B^T+C_P\mathbf{S}_P^T+\mathbf{E} \quad (5)$$

where C_S, , C_B, and C_P represent the concentration profiles of styrene, 1,3-butadiene, and poly(butadiene), respectively, and $\mathbf{S}_S$, $\mathbf{S}_B$, and $\mathbf{S}_P$ represent their pure spectra, respectively.

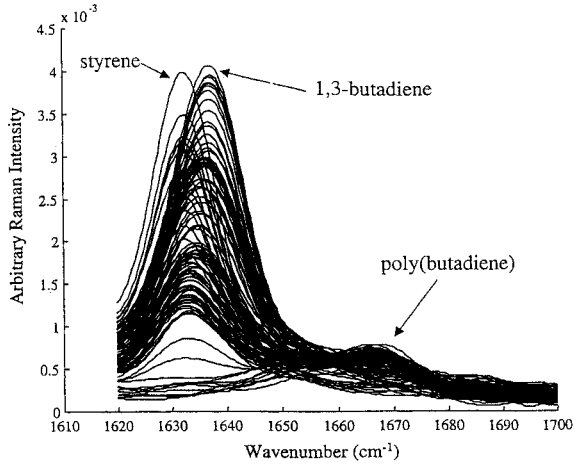

Fig. 1: FT-Raman spectra in the 1700-1620 cm^{-1} region obtained during the blockcopolymerisation of styrene and 1,3-buntadiene. The Raman spectra were obtained with a Bruker IFS66 FT-Raman spectrometer equipped with a Nd:YAG Laser. (Reproduced from ref. 13 with permission. Copyright (2001)Wiley-VCH).

The residuals **E** are minimised in a least squares sense. In an alternating way, first the concentration profiles are estimated that fit the spectra optimally considering an initial estimate of the pure spectra. Based on these estimated concentration profiles, new pure spectra are calculated that optimally fit the spectra. These two steps are repeated until no further improvement in fit is obtained. During the estimations, the concentration profiles and the pure spectra are constrained to be non-negative. Furthermore, profiles can be constrained to monotonically decrease or increase, or only have one maximum (unimodality). Such constraints are often useful for the estimation of concentration profiles, but they were not used in this analysis.

The first step of this study was to separate the first twelve spectra collected before the addition of the 1,3-butadiene from the 102 remaining spectra. The ALS method was employed to calculate the concentration profiles and pure spectra of the chemical species that fit the obtained spectral data.[13] As an initial estimate of the pure spectrum of styrene, the first spectrum was used. Only a few steps of the ALS algorithm yielded the final concentration profile and pure spectrum of styrene.

After the addition of 1,3-butadiene, the continuing polymerisation leads to a decrease of the 1,3-butadiene concentration and an increase of the poly(butadiene) concentration. The styrene is expected to remain almost constant until the 1,3-butadiene has reacted completely. Subsequently, the residual styrene concentration will also decrease to zero. The estimation of pure spectra and concentration profiles became more complicated in the second set of spectra (after the addition of 1,3-butadiene) because the bands due to styrene and 1,3-butadiene overlap severely in the 1640-1630 cm^{-1} region. During the whole SMCR analysis of the second set, the pure spectrum of styrene was fixed to equal the one obtained from the analysis of the spectra in the first step. The pure spectrum of styrene calculated from the SMCR analysis is preferred over the first spectrum, which was obtained before the initiator was added to the styrene mixture, because by combining the twelve spectra of the first step, the noise in the final estimate of the pure spectrum is reduced significantly. For the initial estimate of the pure spectrum of poly(butadiene), the last spectrum acquired from the reaction system was used. The first spectrum obtained after the addition of 1,3-butadiene also contains a considerable contribution from styrene. Because these components show heavily overlapping bands, this contribution of styrene should be removed. Since the concentration of styrene just before the addition of 1,3-butadiene is known from the SMCR analysis of the first set, and also its pure spectrum is known, the total contribution of styrene can be removed from the spectrum obtained directly after 1,3-butadiene is added. This spectrum was used as an initial estimate of the pure spectrum of 1,3-butadiene for the ALS algorithm. For the estimation of all concentration profiles and of the pure spectra of 1,3-butadiene and poly(butadiene), non-negativity constraints were used.

Fig. 2A and B show the final results of the concentration profiles and pure spectra of styrene, 1,3-butadiene and poly(butadiene), respectively. It is noted that

during the first half hour, which was analysed as the first set, only the decrease of styrene is observed. During the polymerisation of 1,3- butadiene, the styrene concentration drops only slowly. This is consistent with the copolymerisation kinetics predicted for styrene in the presence of butadiene. Only after 1,3-butadiene has almost polymerised completely (after about 6 hours), the residual amount of monomeric styrene polymerises very fast to completion, thereby forming the third block of the copolymer. The pure spectra in Fig. 2B delineate the very natural shapes of the spectra, proving that the calculated concentration profiles are realistic. Comparison with reference spectra shows that the modeled pure spectra also agree in terms of the peak wavenumber positions. OPA was also used to model the data and gave similar results.[32]

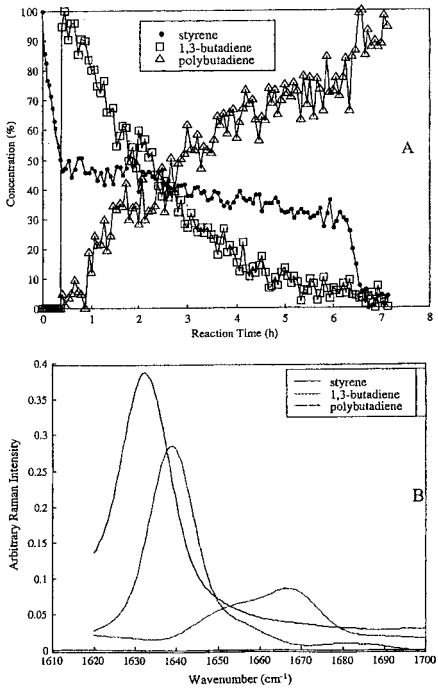

Fig. 2: A. The concentration profiles of styrene, 1,3-butadiene and poly (butadiene). B. The pure spectra of styrene, 1,3-butadiene and poly(butadiene) (Reproduced from ref. 13 with permission. Copyright (2001)Wiley-VCH).

SELF-MODELING CURVE RESOLUTION ANALYSIS OF ON-LINE NIR DATA OF THE MELT EXTRUSION TRANSESTERIFICATION

Šašic et al.[12] reported a SMCR study of the transesterification of molten ethylene/vinylacetate (EVA) copolymers by octanol as a reagent and sodium methoxide as a catalyst in an extruder. Fig. 3 specifies the reaction analyzed in the present study. The reaction product (octylacetate) was evacuated from the extruder and only polymeric product was expected to appear at the exit of the extruder. Octanol was added two minutes after the start of the spectral measurement. There is a time delay between the addition of the reactant and the appearance of the products at the exit of the extruder (residence time). The product appears for the first time several minutes after the start of the reaction. All the time axes in the figures indicate the time after the addition of octanol. A total of 60 NIR spectra were acquired for 37 minutes with the last spectrum recorded 31 minutes after of octanol and catalyst was stopped. They used OPA and multivariate curve resolution (MCR) to resolve the spectra and to derive concentration profiles of the species.[12]

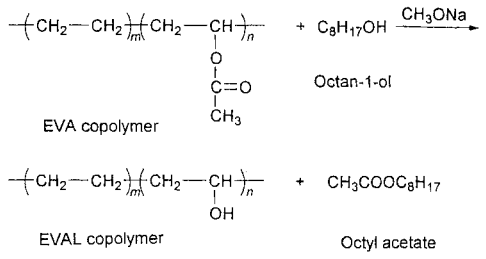

Fig. 3: Transestrification reaction of EVA copolymer (Reproduced from ref. 12 with permission. Copyright (2000) Royal Society of Chemistry).

Fig. 4 shows NIR spectra of the reaction mixture in the regions of 9000-7800 cm^{-1}(A), 7500-6500 cm^{-1}(B) and 5100-4600 cm^{-1}(C).[12] In the 9000-7800 cm^{-1} region one can observe the bands assigned to the second overtones of the C-H stretching vibrations and in the second region (7500-6500 cm^{-1}) those arising from the first overtones of the O-H stretching vibrations and combinations of 2 x C-H stretching and C-H deformation

vibrations appear. The bands observed in the last region are due to a combination of C-H stretching and C=O stretching vibrations and combination modes of CH_2 vibrations.[12]

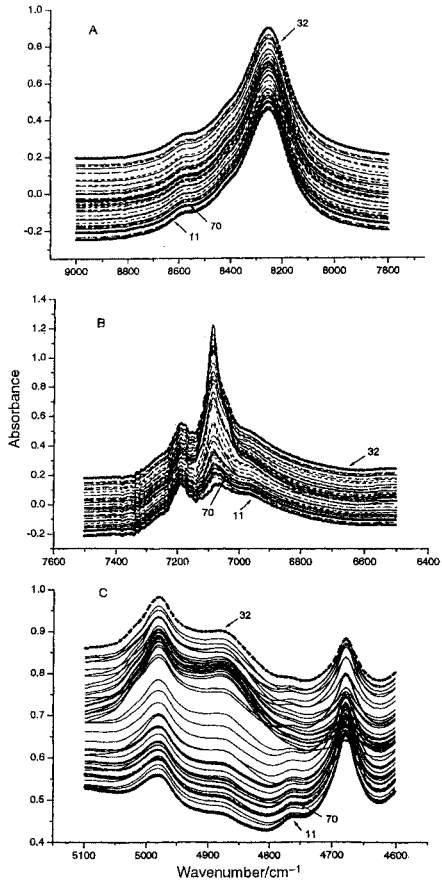

Fig. 4: NIR spectra in the 9000-7800 (A), 7500-6500 (B) and 5100-4600 cm^{-1} regions acquired during the reaction shown in Fig. 3. 11 indicates the first and 70 the last spectrum used for the SMCR analyses (Reproduced from ref. 12 with permission. Copyright (2000) Royal Society of Chemistry).

The spectra Fig. 4 were subjected to multiplicative scattering correction (MSC). The resulting spectra are shown in Fig. 5.[12] The first region changes little with the esterification. It is noted in the second region that the band at 7089 cm^{-1} increases in

concert with the decrease in the bands at 7189 and 6965 cm^{-1}. The spectral changes in the 5100-4600 cm^{-1} region show two isosbestic points at 5033 and 4771 cm^{-1}, implying a simple reaction of two components. The most intense spectrum is the one measured 29 minutes after the reaction started while the last spectrum used in the analysis is very close to the spectrum obtained before the addition of octanol. In this review we discuss only the 7500-6500 cm^{-1} region.

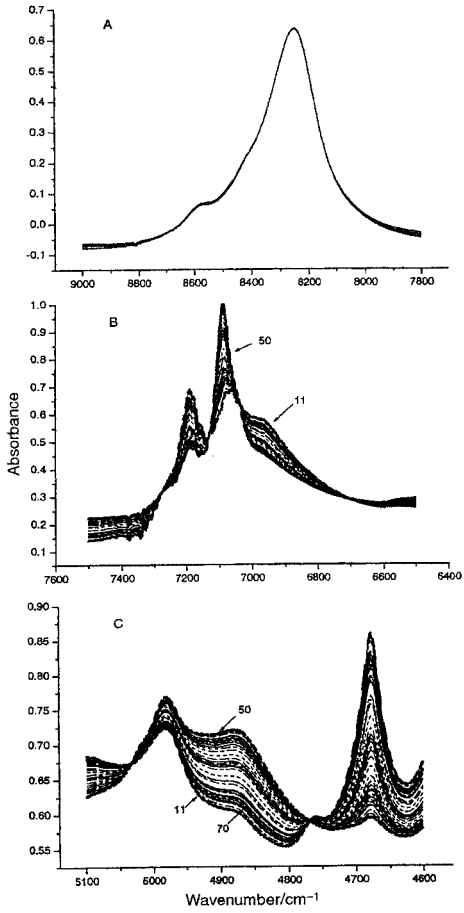

Fig. 5: (A)-(C) NIR spectra from Fig. 4(A)-(C) after MSC (Reproduced from ref. 12 with permission. Copyright (2000) Royal Society of Chemistry).

Rank analysis of the spectra in Fig. 5(B) yields the first two eigenvalues of 255 and 18.2 while rest of eigenvalues are less than 10^4, showing that the system is a two-component system. The first two scores and loadings are shown in Fig. 6.[12] It is of interest that the scores are very much different by intensities. A Rank of two is maintained by OPA. The first three dissimilarity spectra obtained by OPA are shown in Fig. 7. The third dissimilarity spectrum shows much less intensity compared with the first two, indicating that two components are present. the purest variables are seen at 7189 and 7089 cm^{-1}. The intensity changes in these variables are shown in Fig. 8(A).[12] These two lines serve as a first guess of the concentration profiles.

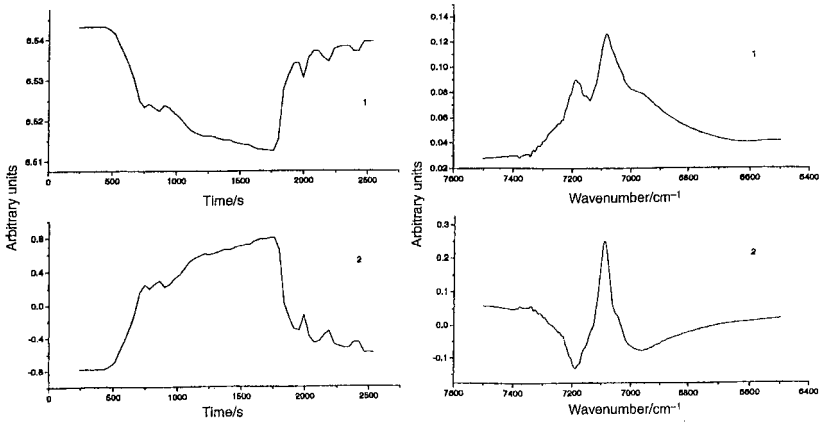

Fig. 6: The first two scores (left) and loading (right) obtained by decomposing the spectra shown in Fig. 5B (Reproduced from ref. 12 with permission. Copyright (2000) Royal Society of Chemistry).

Note that both spectra in Fig. 8(B) show some pitfalls. The spectrum that increases during the reaction has a negative spike at 7189 cm^{-1}, and shows only one strong peak at 7089 cm^{-1} assignable to the first overtone of the O-H vibration of EVAL copolymer. However, looking at the reaction one cannot expect the absence of C-H combination bands for the EVAL copolymer compared to the spectrum of the EVA copolymer. On the other hand, the decreasing component shows a sharp intensity change in the position where the spectrum of EVAL copolymer shows the maximum. Thus, the result derived by OPA does not seem to be correct. It cannot be improved by

using constraints of non-negativity, unimodality or closure of concentration. Applications of these constraints can change only relative intensities of the features in Fig. 8(B) but not their sharps.

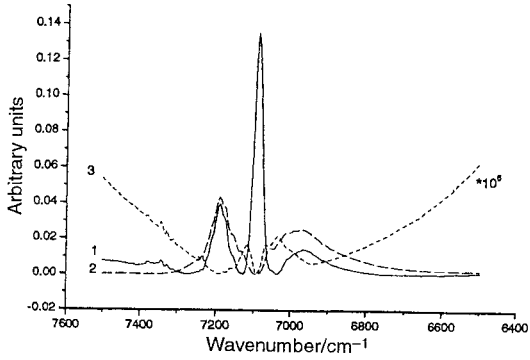

Fig. 7: The first three dissimilarity spectra calculated by OPA (Reproduced from ref. 12 with permission. Copyright (2000) Royal Society of Chemistry).

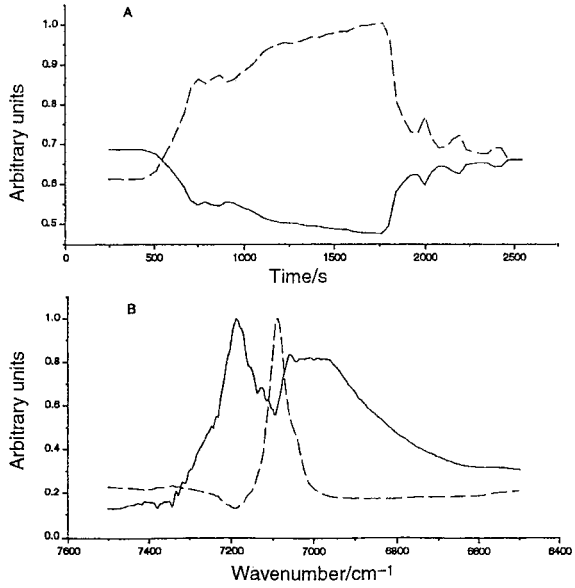

Fig. 8: Intensity changes of pure variables that are found by OPA (A) and the corresponding pure component spectra (B) (Reproduced from ref. 12 with permission. Copyright (2000) Royal Society of Chemistry).

The result obtained by OPA was not unexpected. The band overlapping is too severe and there are apparently no really pure variable. The variable at 7189 cm^{-1} is affected by the spectrum of the EVA copolymer (decreasing component) while the variable at 7089 cm^{-1} is influenced by the EVAL copolymer spectrum because the EVAL copolymer contains OH groups. Therefore, searching for the pure variables does not provide an optimum result.

In conclusion, the study of NIR spectra obtained during the transesterification of EVA copolymer in the extruder provided a good example for the on-line analysis by SMCR methods. By use of the SMCR methods it is possible to monitor the process in real time, to have deep insight into the reaction dynamic and to resolve the spectra of reactant and product.

PARALLEL VECTOR ANALYSIS(PVA)—A NEW POWERFUL SMCR METHOD

The idea of PVA is to construct a set of subspaces comprising only one common (spectral) component and then find a vector that is in parallel with a series of vectors coming from different subspaces.[14-16] With suitably constructed subspaces, the PVA procedure offers a versatile approach to the unique resolution of spectral profiles. A special advantage of PVA is that one can selectively resolve the components of interest without regard to the global bilinear model and other interferents.

The PVA method is based on the theorem that, for M different subspaces $\mathbf{A}_1$, $\mathbf{A}_2$, ..., and $\mathbf{A}_M$ that are generated by a set of linear independent spectral vectors $\mathbf{s}_1$, $\mathbf{s}_2$, ..., $\mathbf{s}_N$, if $\mathbf{s}_1$ belongs to each subspace, and for any other spectral vector $\mathbf{s}_n$ (n = 2, 3, ..., N) there exists a subspace which does not contain $\mathbf{s}_n$, then, if there is a non-zero vector $\mathbf{x}$ belonging to all the subspaces, it must satisfy $\mathbf{x} = k\mathbf{s}_1$ with k being a non-zero constant. This theorem directly leads to the inference that if one can find a set of spectral subspaces that only comprise one common spectra, then the spectra that are common to all subspaces uniquely resolvable. Actually, this theorem is a more generic condition for unique resolution of two-way data than the previous one,[10] and it applies to general situations besides the data from hyphenated chromatography.

The objective of PVA is to seek a vector $\mathbf{x}$ minimizing the following loss function L under the conditions that $\mathbf{x}^T\mathbf{x} = 1$:

$$L(\mathbf{x}, \mathbf{b}_m) = \sum_{m=1}^{M} \| \mathbf{A}_m \mathbf{b}_m - \mathbf{x} \|^2 \tag{6}$$

where $\mathbf{A}_m$ (m = 1, 2, ..., M) is the matrix made up by the base vectors of the corresponding subspace and $\mathbf{b}_m$ is the combination coefficient vector to be optimized. Since the method attempts to seek vectors that come from different subspaces, but are in parallel with each other, this approach is then called as parallel vector analysis (PVA). It can be shown that the solution $\mathbf{x}$ is the first eigenvector (the eigenvector corresponding to the largest eigenvalue) for the following eigen-problem:

$$\sum_{m=1}^{M} \mathbf{A}_m \mathbf{A}_m^{+} \mathbf{x} = \lambda \mathbf{x} \tag{7}$$

Notice that $\mathbf{A}_m\mathbf{A}_m^{+}$ is the projection matrix on the subspace $\mathbf{A}_m$. If there is a vector common to all subspaces, the largest eigenvalue of $\sum_{m=1}^{M} \mathbf{A}_m \mathbf{A}_m^{+}$ is M. Conversely, if one obtains the first eigenvector associated with an eigenvalue very close to M, this eigenvector must belong to all subspaces. This conclusion is consistent with the aim of PVA. Moreover, this conclusion reveals an important fact that one can evaluate the solution using the eigenvalues: If the largest eigenvalue is significantly smaller than M, then there must not be a vector common to all subspaces. If the second largest eigenvalue also shows insignificant difference between M, then there must exist more than one vector belonging to all subspaces. That is, the solution is not unique.

Resolution of reaction profiles by WFA

WFA is derived from another generic theorem for unique resolution that if the spectral subspace for all the interferents that have concentration profiles overlapping that of the analyte is available, then the concentration profile of the analyte is uniquely resolvable.[14] Therefore, the fundamental principle of WFA to find a time window in which the subspace orthogonal to spectra of interfering species or reactions can be estimated. The implementation of WFA in the resolution of reaction systems is slightly

different from the standard one, which is outlined as follows: First, a time window $\mathbf{X}_w$ in which the reaction to be resolved is proceeding is defined. That is, the time window starts from the initiating point of the reaction and ends with the termination of the reaction. Second, one or several time domains $\mathbf{X}_i$ (i = 1, ...) outside the time window $\mathbf{X}_w$ are chosen where the interfering reactions are in active progress. Third, the spectra in each time domain $\mathbf{X}_i$ are separately analyzed by mean-centering window (MCWPCA) to extract the spectral subspace $\mathbf{V}_i$ of reactions active in this time domain. Obviously, one can see that the augmented matrix $\mathbf{V} = (\mathbf{V}_1, ...)$ gives an estimate of the spectral subspace for all the interfering reactions. Fourth, the spectra in the time window $\mathbf{X}_w$ are each subtracted by the first spectra of the window, i. e., all the rows of $\mathbf{X}_w$ are subtracted by the first row of $\mathbf{X}_w$. That is, $\mathbf{Z}_w = \mathbf{X}_w - \mathbf{1}_H \mathbf{x}_w^T$, where $\mathbf{x}_w^T$ is the first row spectra of $\mathbf{X}_w$, and H is the number of rows in $\mathbf{X}_w$. Based on eq (7), one then has

$$\mathbf{Z}_w = \mathbf{X}_w - \mathbf{1}_H \mathbf{x}_w^T = \Xi_w \mathbf{R}_w^T + \mathbf{E}_w \tag{8}$$

Multiplying $\mathbf{Z}_w$ by $(\mathbf{I}_H - (\mathbf{V}^T)^+ \mathbf{V}^T)$ yields

$$\begin{aligned}
&\mathbf{Z}_w (\mathbf{I}_H - (\mathbf{V}^T)^+ \mathbf{V}^T) \\
&\quad = \Xi_w \mathbf{R}_w^T (\mathbf{I}_H - (\mathbf{V}^T)^+ \mathbf{V}^T) + \mathbf{E}_w (\mathbf{I}_H - (\mathbf{V}^T)^+ \mathbf{V}^T) \qquad (9) \\
&\quad = \sum_{k=1}^{K} \xi_k \mathbf{r}_k^T (\mathbf{I}_H - (\mathbf{V}^T)^+ \mathbf{V}^T) + \mathbf{E}_w (\mathbf{I}_H - (\mathbf{V}^T)^+ \mathbf{V}^T) \qquad (10)
\end{aligned}$$

where the superscript $^+$ symbolizes the Penrose-Moore generalized inverse. Because $(\mathbf{I}_H - (\mathbf{V}^T)^+ \mathbf{V}^T)$ is the projection matrix onto the subspace orthogonal to $\mathbf{V}$, which is generated by the spectra of all the other $K_i - 1$ interfering reactions except the reaction to be resolved. Without loss of generality, it can be assumed that the reaction to be resolved is the first one. That is, $(\mathbf{I}_H - (\mathbf{V}^T)^+ \mathbf{V}^T)$ is the projectio

n matrix onto the subspace orthogonal to all $\mathbf{r}_k$'s (k = 2, 3, ..., K). Then one has

$$\mathbf{Z}_w(\mathbf{I}_H - (\mathbf{V}^T)^+ \mathbf{V}^T) = \xi_1 \mathbf{r}_1^T (\mathbf{I}_H - (\mathbf{V}^T)^+ \mathbf{V}^T) + \mathbf{E}_w (\mathbf{I}_H - (\mathbf{V}^T)^+ \mathbf{V}^T) \tag{11}$$

Notice that when (?) the pseudo-rank of $\mathbf{Z}_w$ ($\mathbf{I}_H - (\mathbf{V}^T)^+ \mathbf{V}^T$) is one, then it is inferred that ξ_1 can be estimated by the first left singular vector of $\mathbf{Z}_w$ ($\mathbf{I}_H - (\mathbf{V}^T)^+ \mathbf{V}^T$).

After the extent curves of reactions have been resolved, the concentration profiles can be computed and other information provided by fixed-sized window evolving factor analysis (FSWEFA) or mean-centering window evolving factor analysis (MCWEFA). PVA may be a very competitive procedure for self-modelling curve resolution of two-way data, especially in situations where the selective regions are not easily available in two directions. As a matter of fact, PVA and WFA are intrinsically two complementary methods: PVA is an approach for the resolution of spectral profiles, while WFA is a method for resolving the concentration profiles.

REFERENCES

1. J. M. Chalmers, ed. *Spectroscopy in Process Analysis,* Sheffield Academic Press; Sheffield, **2000.**
2. J. B. Cooper, in *Analytical Applications of Raman Spectroscopy,* M. J. Pelletier ed., Blackwell Science, Oxford, **1999**, p.193.
3. Y. Ozaki and T. Amari, in ref. 1, p. 53.
4. J. J. Workman, Jr. *Appl. Spectrosc. Rev.* **1999**, *34*, 1.
5. N. J. Everall, in *An Introduction to Laser Spectroscopy*, D. L. Andrews and A. A. Demidov, eds., Plenum Press, New York, **1995**, p.115.
6. R. Tauler, B. R. Kowalski, and S. Fleming, *Anal. Chem.* **1998**, *65*, 2040.
7. R. Tauler, A. K. Smilde, J. M. Henshaw, L. W. Burgess, and B. R. Kowalski, *Anal. Chem.* **1994**, *66*, 3337.
8. A. C. Quinn, P. J. Gemperline, B. Baker, M. Zhu, D. S Walker, and *Chemom. Intell. Lab. Syst.* **1999**, *45*, 199.
9. P. J. Gemperline, *Anal. Chem.* **1999**, *69*, 5398.
10. R. Manne, *Chemom. Intell. Lab. Syst.* **1995**, *27*, 89.
11. B. G. M. Vandenginste, D. L. Massart, L. M. C. Buydens, S. de Jong, P. J. Lewi and J. Smeyers-Verbecke, *Handbook of Chemometrics and Qualimetrics,* Elsevier, Amsterdam, **1998**.
12. S. Šašić, Y. Kita, T. Furukawa, H. W. Siesler, and Y. Ozaki, *Analyst*, **2000**, *125*, 2315.

13. F. Bandermann, I. Tausendfreund, S. Šašic. Y. Ozaki, M. Kleimann, J. A. Westerhuins, and H. W. Siesler, *Macromol. Rapid Comm.* **2001,** 22, 690.
14. J.-H. Jiang, S. Šašić, R.-Q. Yu, and Y. Ozaki, Submitted to *Anal. Chem.*
15. J.-H. Jiang, M. Kleimann, H. W. Siesler, and Y. Ozaki, Submitted to *Anal. Chem.*
16. J.-H. Jiang, and Y. Ozaki, *Anal. Sci.* in press.
17. M. Maeder, *Anal. Chem.* **1987**, *59*, 527.
18. E. R. Malinowski, *J. Chemom.* **1992**, *6*, 29
19. O. M. Kvalheim, and Y. Z. Liang, *Anal. Chem.* **1992**, *64*, 936.
20. Y. Z. Liang, and O. M. Kvalheim, *Chemom. Intell. Lab. Syst.* **1993**, *20*, 115.
21. R. Manne, H. L. Shen, and Y. Z. Liang, *Chemom. Intell. Lab. Syst.* **1999**, *45*, 171.
22. F. Cuesta Sanchez, B. van den Bogaert, S. C. Rutan, and D. L. Massart, *Chemom. Intell. Lab. Syst.* **1996**, *34*, 139.
23. K. deBraekeleer and D. L. Massart, *Chemom. Intell. Lab. Syst.* **1997**, *39*, 127.
24. W. Windig and J. Guilment, *Anal. Chem.* **1991**, *63*, 1425.
25. W. Windig, *Chemom. Intell. Lab. Syst.* **1997**, *36*, 3
26. P. J. Gemperline, *J. Chem. Inf. Comput. Sci.* **1984**, *24*, 206.
27. B. G. M. Vandeginste, W. Derks, and G. Kateman, *Anal. Chim. Acta*, **1985**, *173*, 253.
28. P. Paatero, *Chemom. Intell. Lab. Syst.* **1997**, *37*, 23.
29. R. Tauler, I. Marques, and E. Casassas, *J. Chemom.* **1998**, *12*, 55.
30. R. Manne, and B. Grande, *Chemom. Intell. Lab. Syst.* **2000**, *50*, 35.
31. I. Tausendfreund, PhD-Thesis, University of Essen, Germany, **2000**.
32. S. Šašić. Y. Ozaki, M. Kleimann, and H. W. Siesler, submitted for publication.